SUPPLEMENTAL MATERIAL

Supplemental Methods

Flow cytometry for detection of endothelial subpopulation markers

Aortas were harvested from four mice and enzymatically digested with collagenase and elastase as described above. Single cell suspensions were stained with Brilliant Violet 421 anti-mouse Cd31 (Biolegend), APC anti-mouse Cd36 (Biolegend), and FITC anti-mouse Vcam1 (Biolegend), and separately with isotype controls for each antibody. The Cd31 positive population was gated for analysis of Cd36 and Vcam1 expression in aortic ECs on a Cytoflex LX flow cytometer (Beckman Coulter).

Immunofluorescence of en face aorta

Mice were euthanized and perfused with 15 ml of 4% ice cold paraformaldehyde. Aortas were harvested from the root to the descending aorta and dissected longitudinally for en face immunofluorescence. Blocking and permeabilization were performed in 1x Dulbecco's Phosphate-Buffered Saline (DPBS) with 1% bovine serum albumin (BSA), 5% donkey serum, 0.1% Tween 20 and 0.1 % Triton X-100 (block buffer) for four hours at 4ºC. Primary antibodies were diluted in block buffer and incubated overnight at 4ºC targeting VE-Cadherin (Cell Signaling Technology), Vcam1 (Cell Signaling Technology) and Cd36 (Abcam). Secondary antibodies labelled with Alexa488, Alexa594 and Alexa647 (Thermo Fisher Scientific) were diluted in the block buffer and incubated for 45 minutes at room temperature. The DAPI stained (1:10000 in PBS) aorta was mounted with the endothelial surface en face.

Fluorescent imaging and image quantification

Confocal image acquisition for fluorescence quantification was performed using an automated Opera Phenix High-Content Screening System (PerkinElmer) with 20x magnification and 1 µM thickness per stack. All the images were acquired on the same day and with same fluorescence parameters. Fluorescence quantification was performed using Harmony High-Content Imaging and Analysis Software (PerkinElmer). 20x images tiled across the specimen were used to reconstruct the whole slide. Nuclei were identified via DAPI staining and vascular smooth muscle cell nuclei were excluded using roundness (≥ 0.7) and area (≥ 50 μm^2) parameters on the image stacks demonstrating VE-Cadherin-targeted antibody fluorescence. Mean intensity of Vcam1 and Cd36-targeted antibody fluorescence were measured in a radius of 10 pixels around the nuclei on the plane of interest.

Autofluorescence from fat cells was removed by excluding fluorescence signals with an intensity z-score>5. To generate spatial maps of fluorescence signal, mean fluorescence for each cell was plotted on X and Y coordinates using the R software package. Vcam1 and Cd36 expression were quantified in each cell from two representative 20x high power field images taken from the aortic greater and lesser curvatures. For each aortic region, the ratio of Vcam1-associated fluorescence to Cd36-associated fluorescence was obtained from three separate aortic root samples, log-transformed, and compared using the Wilcoxon rank-sum test.

Computational Analysis

Pre-processing of droplet-based scRNA-seq data.

De-multiplexing, alignment to the mm10 transcriptome and unique molecular identifier (UMI)-collapsing were performed using the Cellranger toolkit (version 2.1.0)

provided by 10X Genomics. The output was a corrected expression matrix, which was used as an input for further analysis.

Transcription factor target scores

Targets for transcription factors of interest were identified using Version 2 of the TRRUST database[1]. To capture the net effect on expression of targets for a given transcription factor, gene set scores were computed for all cells for gene sets comprising known targets of TF activation. Gene set scores were computed using the Seurat AddModuleScore function as previously described[2]. Briefly, a background gene set was created for each signature gene set by selecting the 10n nearest neighbors to the signature set genes as determined by mean expression and detection frequency in all cells. For each cell, the gene set score was defined as the mean expression of the genes in the signature set minus the mean expression of the background set genes. Significant differences in gene set score distributions between subpopulations were determined using the Mann-Whitney U-test in R.

Integrated analysis of normal and high-fat diet scRNA-seq data

Aortic single cell RNA-seq datasets from normal and high-fat diet fed mice were combined using established methods for combined analysis of two single cell data sets in Seurat[3]. Briefly, this approach uses canonical correlation analysis (CCA) to identify similarities between the datasets and PCA to identify differences. The Seurat RunCCA function generates shared canonical ‘basis’ vectors which captured shared correlation. These basis vectors were aligned using Seurat functions to generate a unified aligned low-dimensional space representing both data sets. Subpopulations shared between the two datasets were identified using the Seurat FindClusters function as previously

described using the top 15 canonical correlates from CCA and a resolution of 0.5. Markers of each subpopulation were identified as previously described using Seurat. In order to identify condition-specific genes that varied between datasets, the FindMarkers function was applied to unaligned data in a low-dimensional space defined by PCA as previously described.

1. Han H, Cho J-W, Lee S, Yun A, Kim H, Bae D, Yang S, Kim CY, Lee M, Kim E, Lee S, Kang B, Jeong D, Kim Y, Jeon H-N, Jung H, Nam S, Chung M, Kim J-H, Lee I. TRRUST v2: an expanded reference database of human and mouse transcriptional regulatory interactions. *Nucleic Acids Res*. 2018;46:D380–D386.

2. Tirosh I, Izar B, Prakadan SM, Wadsworth MH, Treacy D, Trombetta JJ, Rotem A, Rodman C, Lian C, Murphy G, Fallahi-Sichani M, Dutton-Regester K, Lin J-R, Cohen O, Shah P, Lu D, Genshaft AS, Hughes TK, Ziegler CGK, Kazer SW, Gaillard A, Kolb KE, Villani A-C, Johannessen CM, Andreev AY, Van Allen EM, Bertagnolli M, Sorger PK, Sullivan RJ, Flaherty KT, Frederick DT, Jané-Valbuena J, Yoon CH, Rozenblatt-Rosen O, Shalek AK, Regev A, Garraway LA. Dissecting the multicellular ecosystem of metastatic melanoma by single-cell RNA-seq. *Science*. 2016;352:189–196.

3. Butler A, Hoffman P, Smibert P, Papalexi E, Satija R. Integrating single-cell transcriptomic data across different conditions, technologies, and species. *Nat Biotech*. 2018;36:411–420.

Supplemental Table 1: Aortic cell type markers

Cell Type	Marker Gene(s)
Fibroblasts	Pdgfra
VSMC	Cnn1, Myh11
EC	Cdh5
Monocytes	Cd68, Cd115, Lyz2
T/B cells	Cd3d, Cd19
Macrophage/DC	H2-Ab1 (MHC-II), Cd68
RBC	Hbb

Markers used to identify aortic cell types.

Supplemental Table 2: Markers differentiating aortic monocytes and macrophages

	p_val	avg_logFC	% monocytes	% Macrophages	p_val_adj
Cd52	3.40E-152	-1.98	0.338	0.987	5.92E-148
Sepp1	1.13E-149	2.77	0.998	0.462	1.97E-145
Pf4	6.65E-147	3.16	0.987	0.144	1.16E-142
Napsa	2.17E-145	-1.64	0.008	0.628	3.77E-141
Apoe	5.74E-143	2.90	0.997	0.429	9.99E-139
Ear2	2.01E-141	-2.50	0.004	0.599	3.50E-137
Lsp1	5.07E-138	-1.76	0.234	0.936	8.82E-134
C1qa	7.15E-138	2.19	1	0.244	1.25E-133
Tmsb10	9.92E-136	-2.04	0.248	0.92	1.73E-131
C1qc	1.08E-132	2.11	0.998	0.205	1.88E-128
Lgals3	7.96E-130	-1.75	0.24	0.929	1.39E-125
Itm2b	2.32E-127	1.32	0.998	0.933	4.05E-123
Ccr2	1.59E-126	-1.45	0.039	0.657	2.76E-122
C1qb	3.43E-121	1.83	1	0.292	5.98E-117
H2-DMb2	9.19E-120	-1.38	0.007	0.532	1.60E-115
Maf	1.25E-113	2.04	0.882	0.106	2.18E-109
Ninj1	4.84E-113	2.32	0.879	0.183	8.43E-109
Ctsb	3.57E-112	1.43	0.985	0.676	6.22E-108
Mrc1	7.72E-110	1.81	0.92	0.353	1.34E-105
Ltb4r1	2.28E-109	-1.20	0.003	0.478	3.97E-105
Cbr2	3.22E-109	2.20	0.847	0.08	5.60E-105
F13a1	3.45E-107	1.88	0.914	0.292	6.01E-103
Folr2	2.45E-106	2.67	0.806	0.019	4.27E-102
Lyve1	3.48E-106	2.59	0.806	0.019	6.06E-102
Csf1r	1.39E-105	1.53	0.935	0.372	2.42E-101
Actg1	2.86E-103	-1.08	0.898	0.997	4.97E-99
Gm2a	4.94E-99	-1.51	0.281	0.859	8.60E-95
Ms4a6b	3.22E-97	1.76	0.85	0.183	5.61E-93
H2-DMb1	7.45E-95	-1.35	0.316	0.881	1.30E-90
Ftl1	3.85E-94	0.72	1	1	6.70E-90
Coro1a	5.83E-94	-1.19	0.476	0.952	1.02E-89
H2-DMa	2.06E-92	-1.38	0.498	0.913	3.58E-88
Tmsb4x	4.58E-92	-0.55	1	0.997	7.98E-88
Glul	2.64E-91	1.53	0.869	0.365	4.61E-87
Bcl2a1d	3.70E-91	-0.96	0.01	0.433	6.45E-87
Plbd1	5.11E-91	-1.33	0.072	0.596	8.89E-87
Cd63	1.56E-88	1.44	0.893	0.285	2.71E-84
Lgmn	1.01E-87	1.40	0.891	0.298	1.77E-83
Cd24a	2.91E-85	-1.16	0.011	0.41	5.07E-81
Gas6	1.13E-84	1.78	0.74	0.083	1.97E-80
Rplp0	1.36E-84	-0.82	0.949	0.981	2.37E-80
Id2	1.90E-84	-1.35	0.088	0.603	3.30E-80
Ifitm2	4.56E-82	1.15	0.947	0.676	7.94E-78
Trf	7.13E-82	1.26	0.924	0.494	1.24E-77

Markers differentiating aortic monocytes and macrophages. Columns correspond to gene name (Gene), unadjusted p-value of Wilcoxon rank sum test (p_val), average log fold change in monocytes vs. macrophages (avg_logFC), percent of monocytes expressing gene (% Monocytes), percent of macrophages expressing gene (% Macrophages), and Bonferroni-corrected p-value (p_val_adj).

Supplemental Table 3: GO set-based gene lists

Development	Differentiation
Add1	Acvr1
Arhgef26	Acvr2b
Ccm2	Acvrl1
Cdh5	Add1
Cldn1	Alox12
Cldn5	Apold1
Clic4	Arhgef26
Col18a1	Atoh8
Ctnnb1	Bmp4
Dmd	Bmp6
Eng	Bmper
Ezr	Bmpr2
F11r	Btg1
F2rl1	Ccm2
Gpx1	Cdh5
Gstm3	Ceacam1
Heg1	Cldn1
Icam1	Cldn5
Id1	Clic4
Ikbkb	Col18a1
Il1b	Ctnnb1
Marveld2	Dll1
Met	Dmd
Msn	Edf1
Myadm	Eng
Myd88	Ezr
Notch4	F11r
Pde2a	F2rl1
Pde4d	Gdf2
Pecam1	Gpx1
Plod3	Gstm3
Ppp1r16b	Heg1
Ptprs	Hey1
Rap1a	Hey2
Rap1b	Hoxb5
Rap2c	Icam1
Rapgef1	Id1
Rapgef2	Ikbkb
Rapgef3	Il1b
Rdx	Jag1
Rock1	Kdm6b
Rock2	Lama5
S1pr2	Marveld2
S1pr3	Met
Sox18	Msn
Stc1	Myadm
Tjp1	Myd88
Tjp2	Notch1
Tnf	Notch4
Tnfrsf1a	Nr2f2
Tnmd	Nrg1
Vezf1	Nrp1
	Pde2a
	Pde4d
	Pdpn
	Pecam1
	Plod3
	Ppp1r16b
	Prox1
	Prox2
	Ptn
	Ptprs
	Rap1a
	Rap1b
	Rap2c
	Rapgef1
	Rapgef2
	Rapgef3
	Rbpj
	Rdx
	Rock1
	Rock2
	S1pr1
	S1pr2
	S1pr3
	Scube1
	Smad4
	Sox17
	Sox18
	Stc1
	Tjp1
	Tjp2
	Tmem100
	Tnf
	Tnfrsf1a
	Tnmd
	Vezf1
	Xdh
	Zeb1

List of genes used to define GO geneset-based scores in ECs.

Supplemental Table 4: EC subpopulation pathway signature gene lists

ECM Organization	Integrin Signaling	Lipoprotein Handling
Bgn	Vcam1	Gpihbp1
Vcam1	Fn1	Lpl
Mfap5	Thbs1	Scarb1
Bmp4	Col4a3	Mylip
Fn1	Icam1	Angptl4
Lox		Apoc1
Pcolce2		Pltp
Fbln5		
Efemp1		
Thbs1		
Col4a3		
Col5a2		
Icam1		
Col8a1		
Dcn		

List of genes used to define EC subpopulation pathway signature scores

Supplemental Table 5: Tip identity gene list

Tip Genes
Nrp2
Cxcr4
Cd34
Dll4
Apln
Kdr
Plxnd1
Unc5b
Efnb2
Angpt2
Nrp1
Robo4
Flt4
Pdgfb

List of genes used to define tip identity score in ECs.

Supplemental Figure 1

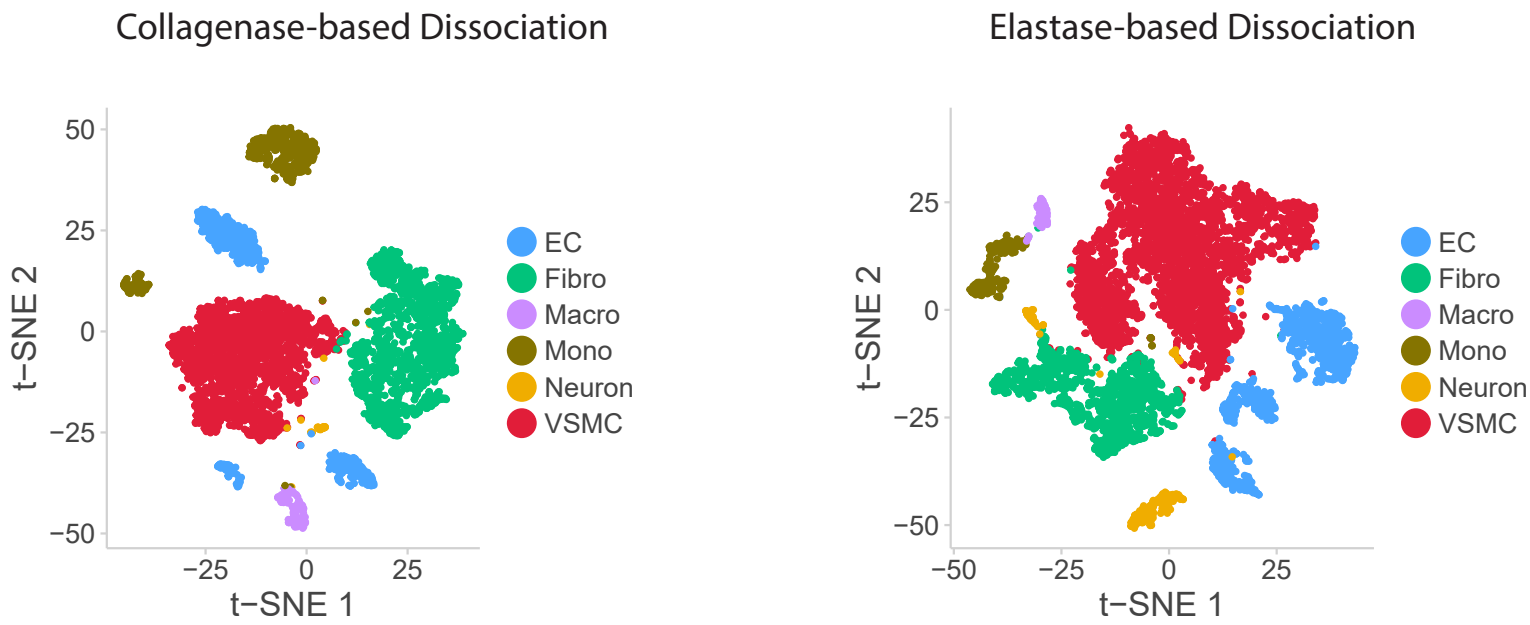

Supplemental Figure 2

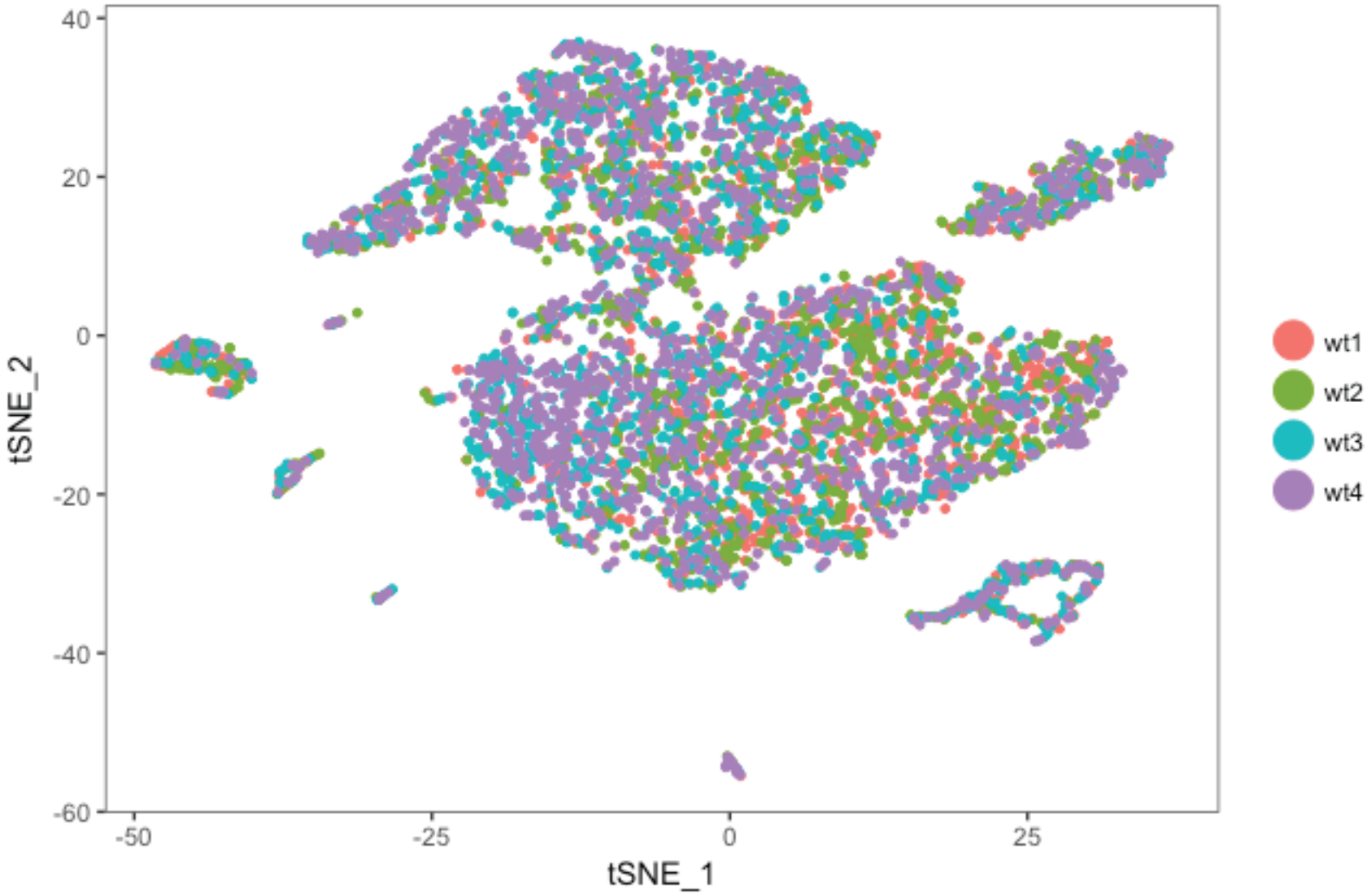

Supplemental Figure 3

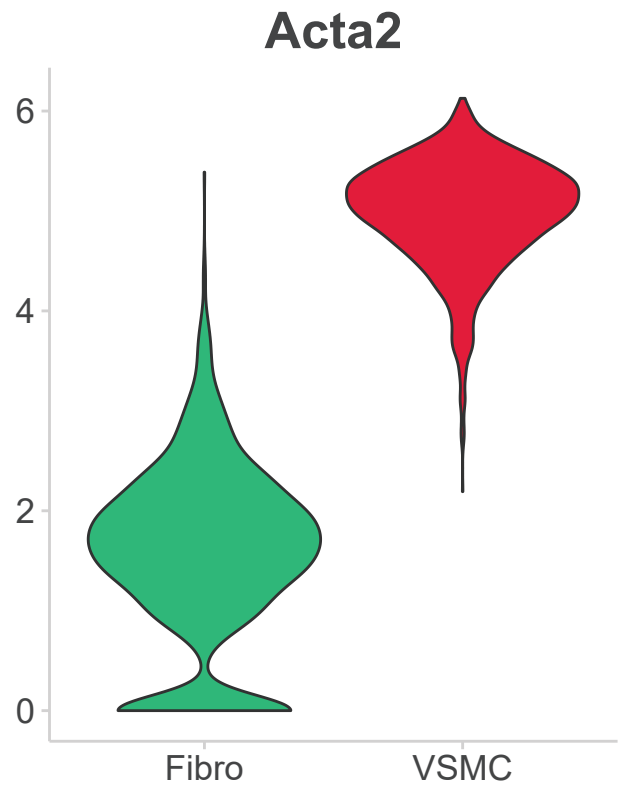

Supplemental Figure 4

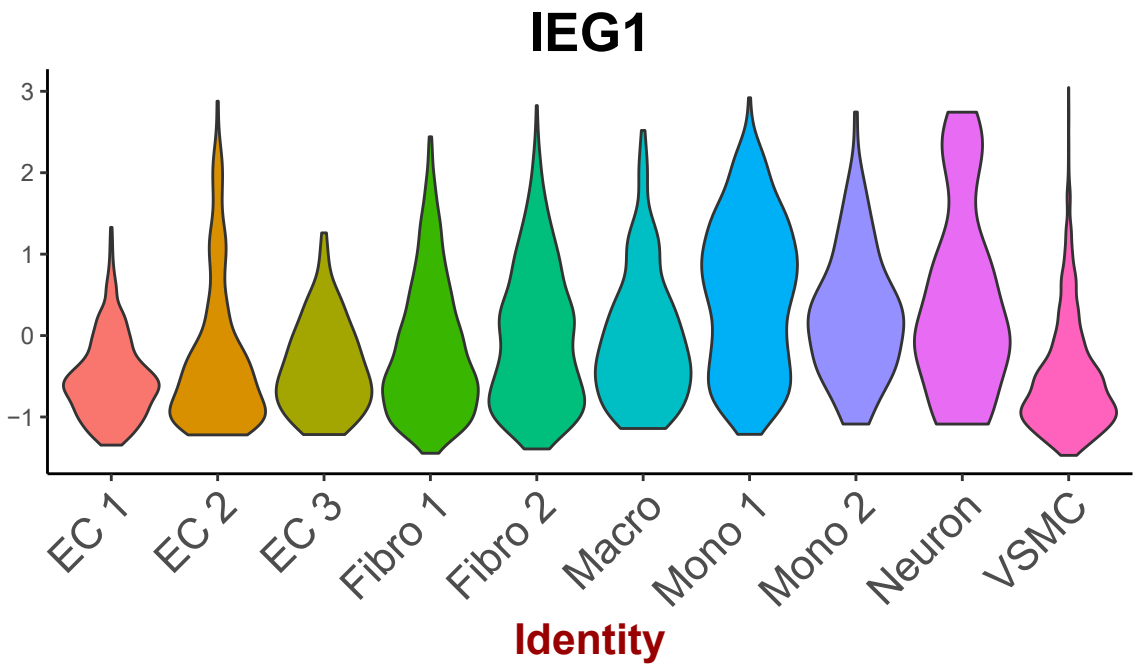

Supplemental Figure 5

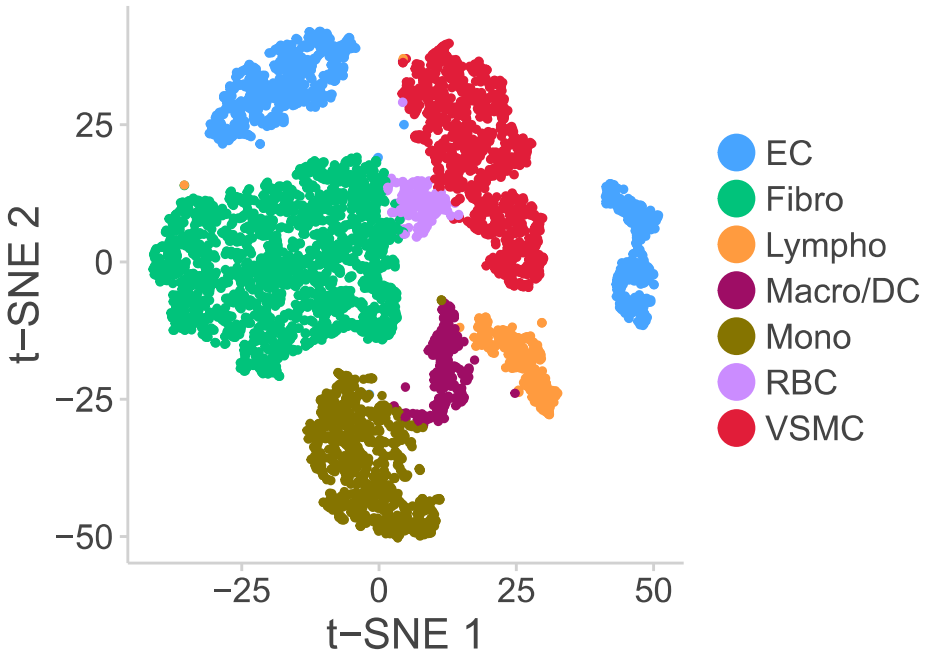

Supplemental Figure 6

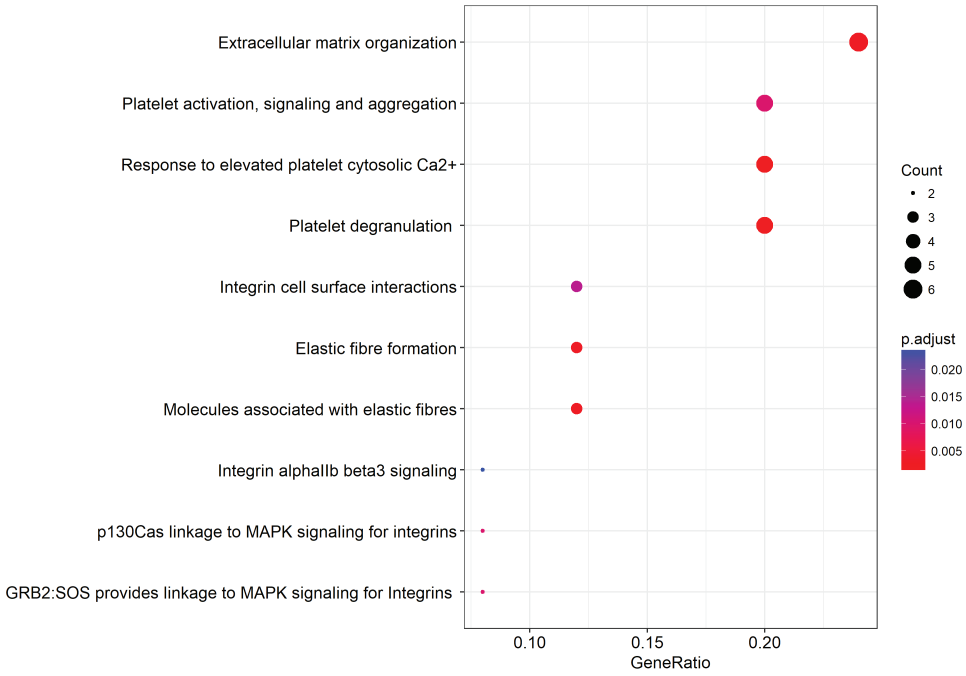

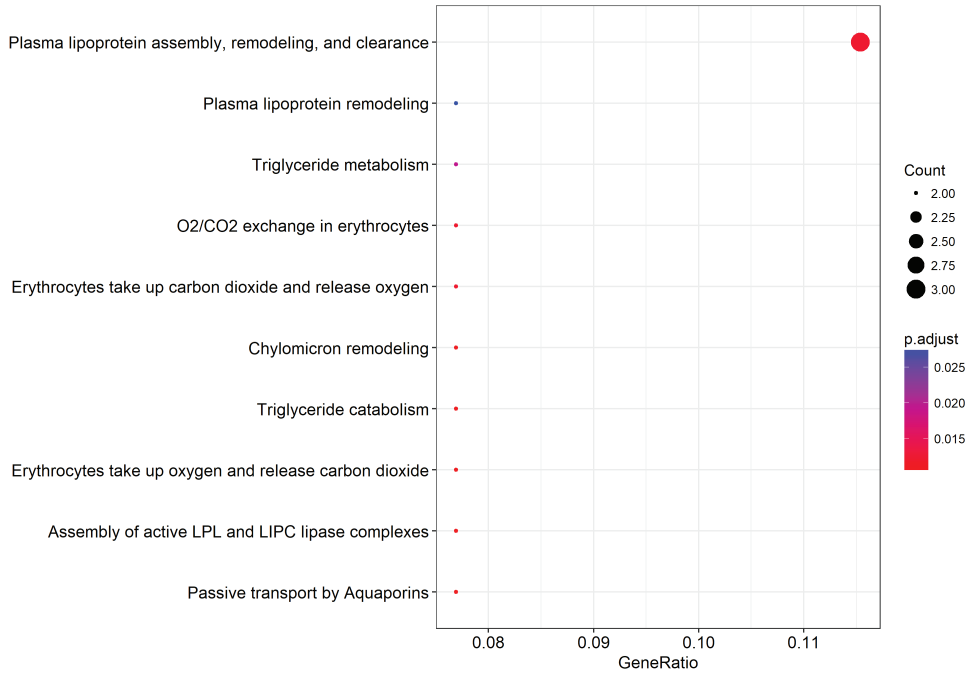

Supplemental Figure 7

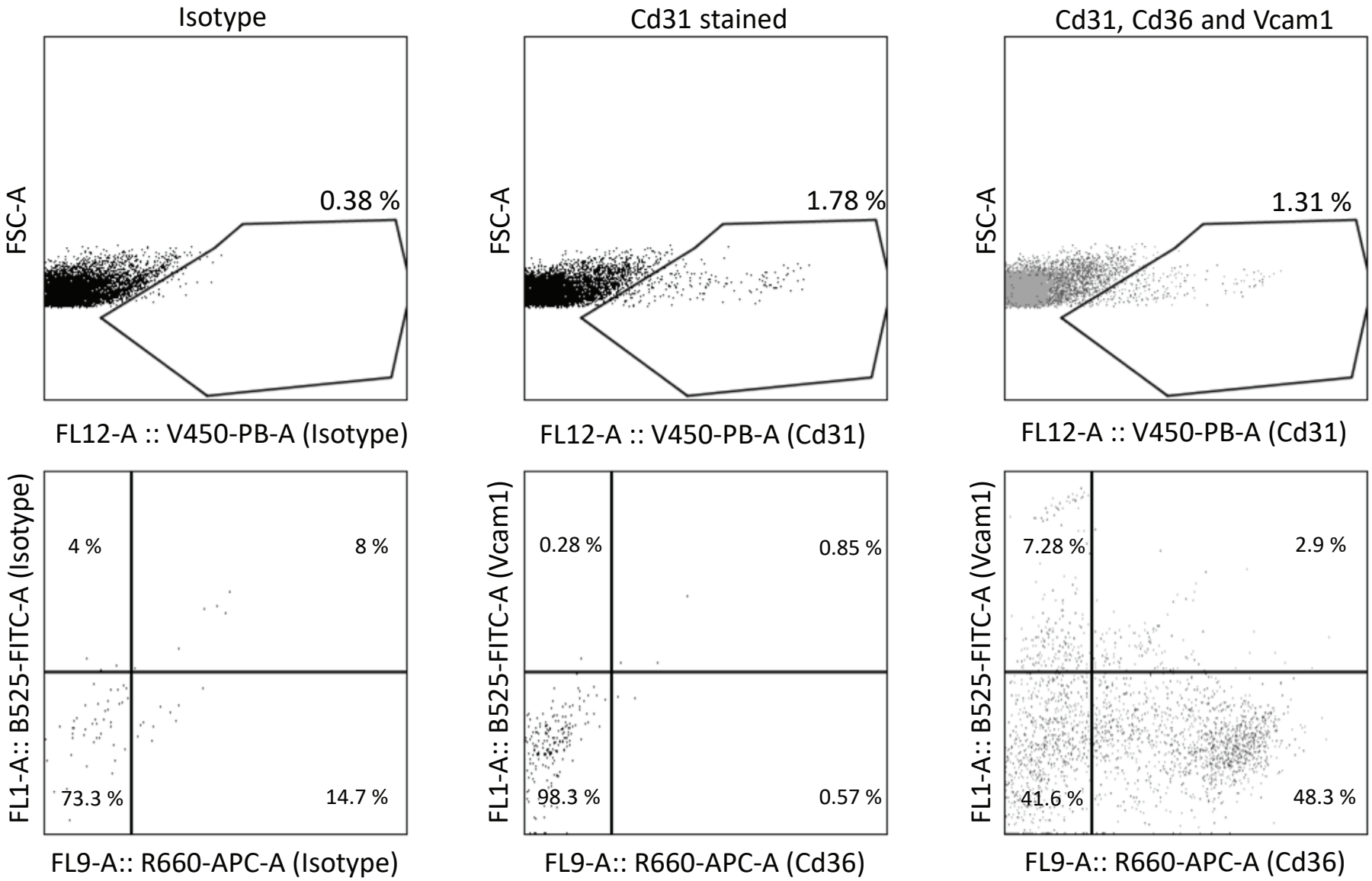

Supplemental Figure 8

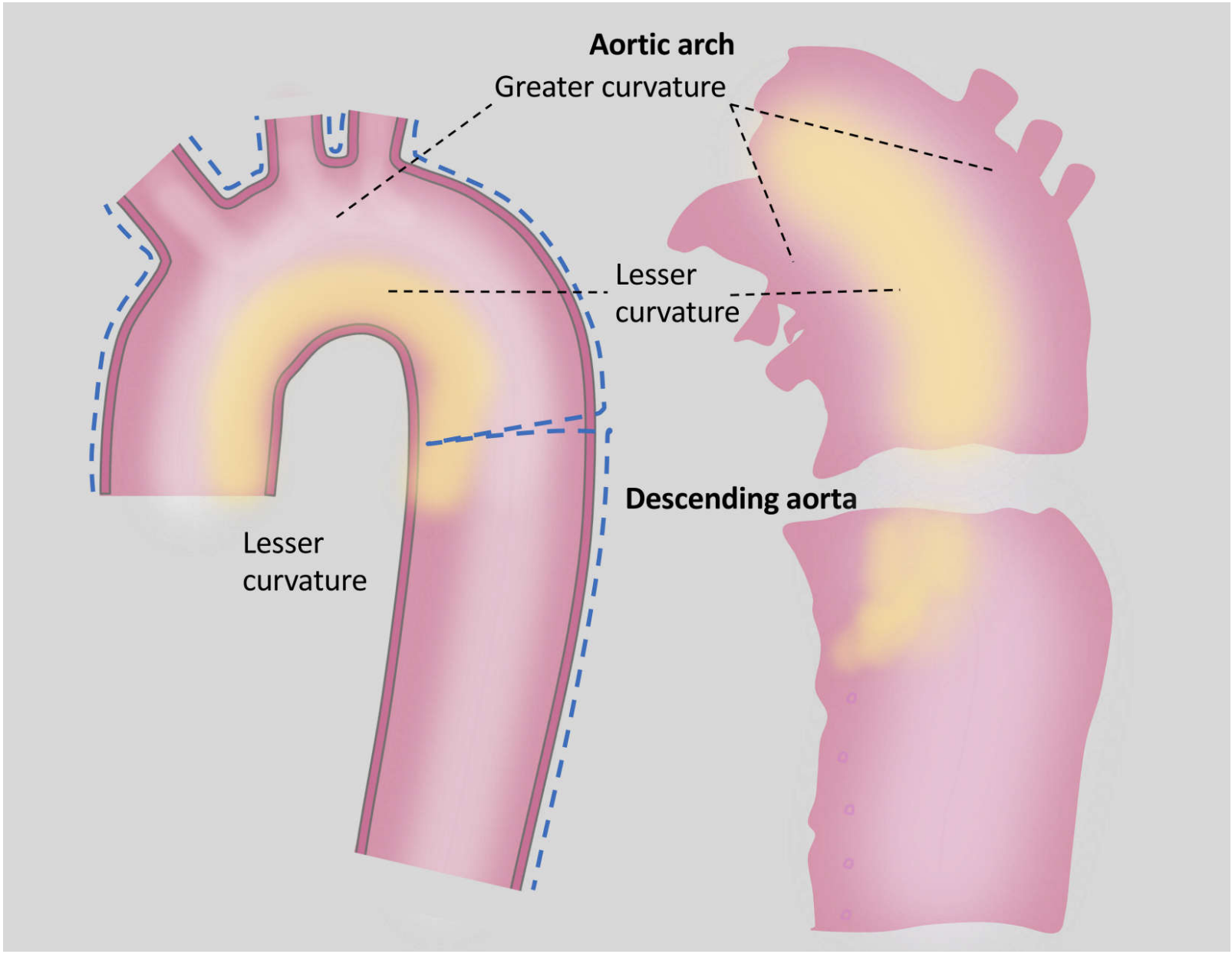

Supplemental Figure 9

a

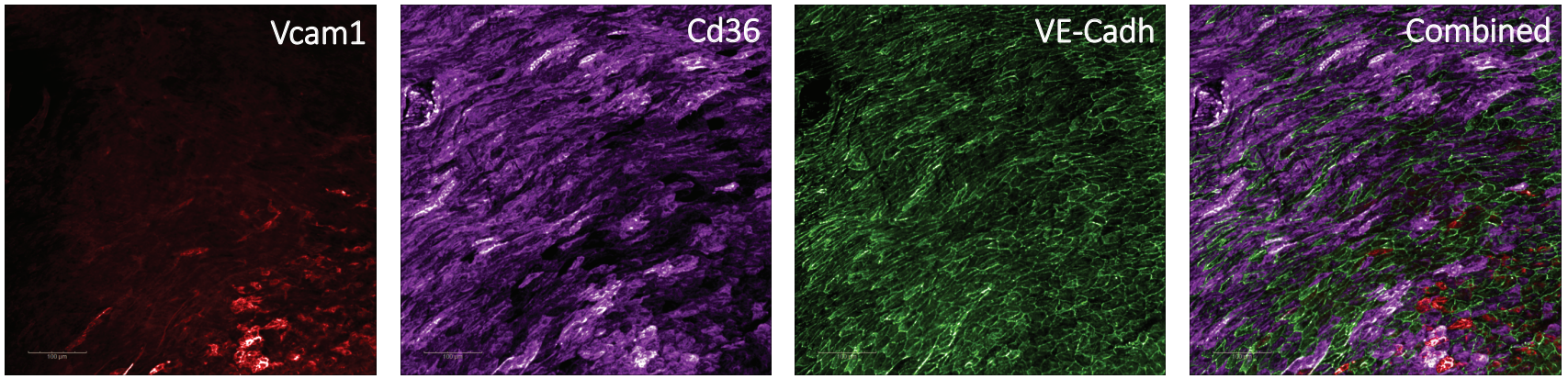

b

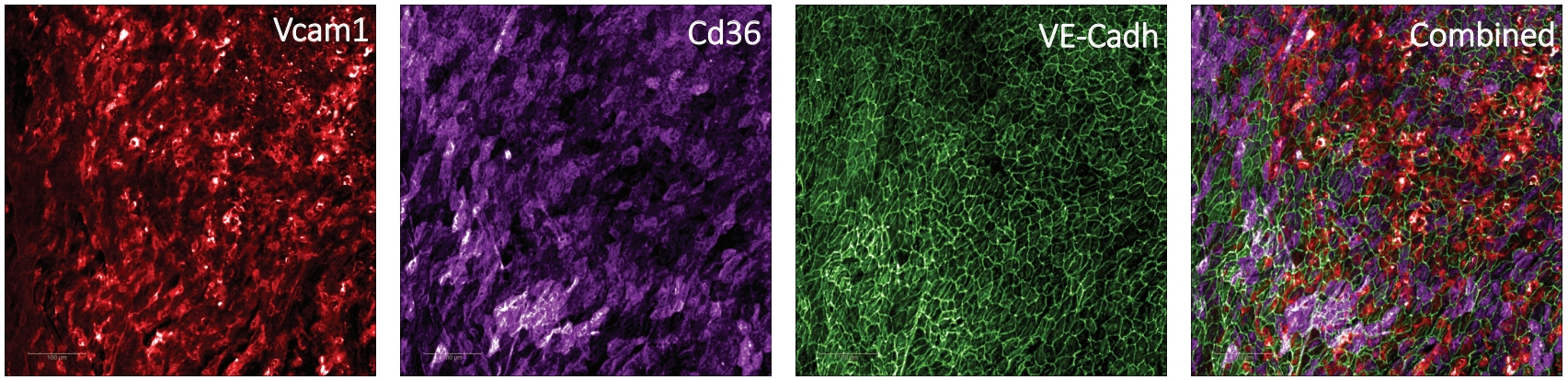

Supplemental Figure 10

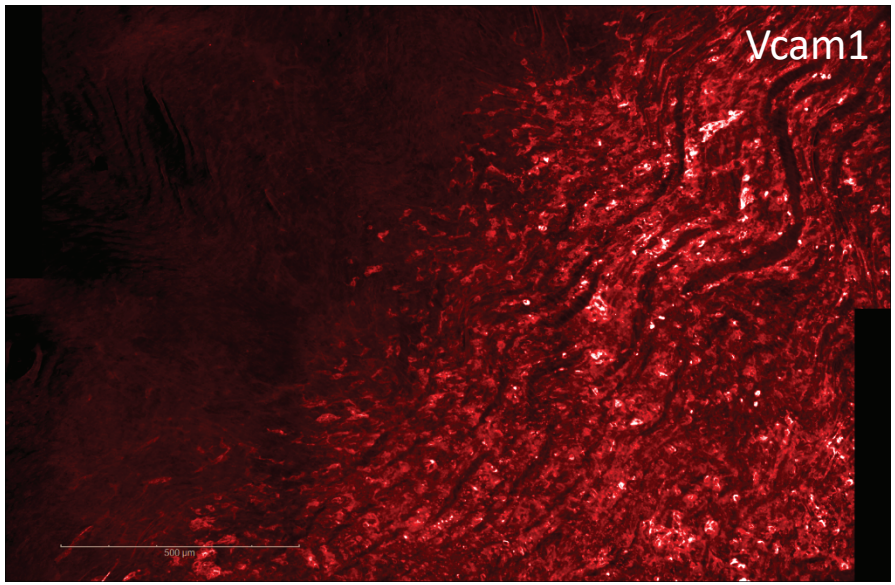

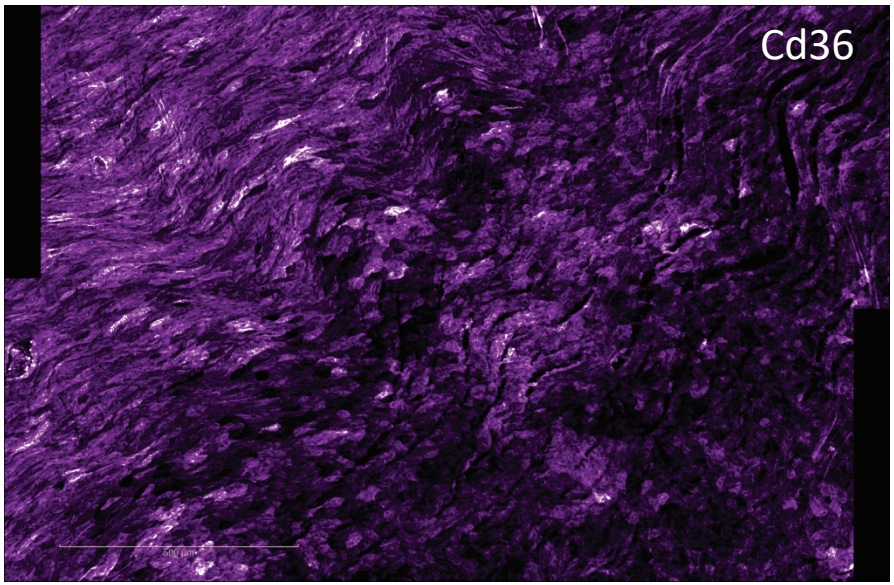

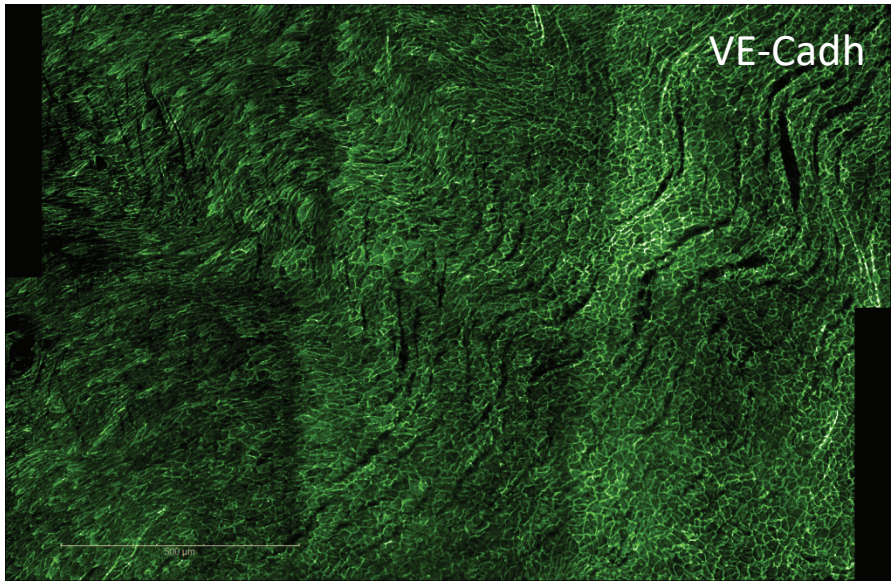

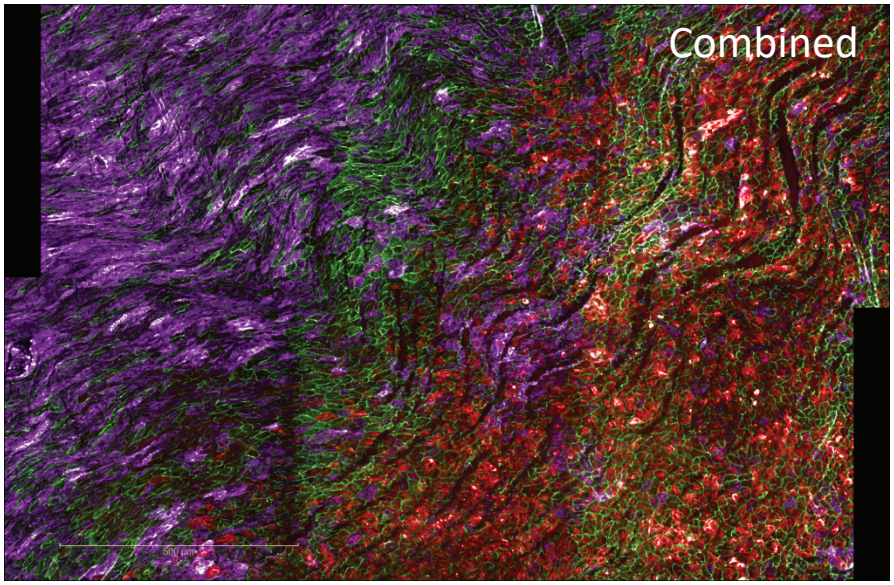

Supplemental Figure Legends

Supplemental Figure 1: Comparison of collagenase/hyaluronidase/DNAse dissociation protocol (original, left) with elastase/collagenase dissociation protocol (right). t-SNE plots summarizing single-cell RNA-seq profiles for each protocol with vascular cell populations labeled. EC indicates endothelial cells; Fibro, fibroblasts; Macro, macrophages; Mono, monocytes; VSMC, vascular smooth muscle cells.

Supplemental Figure 2: t-SNE demonstrating contribution of all analyzed mice to each subpopulation in the overall scRNA-seq profile of the aorta. scRNA-seq profiling of 4 wild-type mouse aortas (wt1-4) demonstrates that subpopulation clustering is not a function of sample origin, and that all samples contribute to all transcriptionally identified populations.

Supplemental Figure 3: Acta2 expression in aortic fibroblasts vs. VSMCs. Violin plot demonstrates increased expression of Acta2 in aortic VSMCs relative to aortic fibroblasts, but nonzero expression in both populations. Violin plot y-axis demonstrates normalized transcript expression values. Fibro indicates fibroblasts; VSMC, vascular smooth muscle cells.

Supplemental Figure 4: Immediate-early gene (IEG; Fos, Fosb, Jun, Junb) activation score for aortic cellular subpopulations. Immediate-early gene activation score does not differentiate the 3 EC subpopulations identified in this study, and these genes are minimally expressed (scores < 0) in aortic ECs, VSMCs, and fibroblasts. EC indicates endothelial cells; Fibro, fibroblasts; Macro, macrophages; Mono, monocytes; VSMC, vascular smooth muscle cells.

Supplemental Figure 5: Resolution of major aortic cell types using lower-depth sc-RNAseq. Seurat clustering analysis pipeline applied to low-depth (17k reads/cell) scRNA-seq library demonstrates resolution of the same major aortic cell populations, including 3 distinct EC populations. EC indicates endothelial cells; Fibro, fibroblasts; Macro, macrophages; Mono, monocytes; VSMC, vascular smooth muscle cells.

Supplemental Figure 6: Reactome pathway enrichment for the top 50 markers of EC 1 (left) and EC 2 (right) using R package ReactomePA. Dot size indicates number of marker genes included in pathway and dot color indicates Benjamini-Hochberg adjusted p-value. Reactome pathways with adjusted p-values < 0.05 are displayed.

Supplemental Figure 7: Gating protocol for FACS analysis of Vcam1 and Cd36 expression in aortic endothelial cells.

Supplemental Figure 8: Schematic representation of aortic root, descending aorta, and lesser and greater curvature regions.

Supplemental Figure 9: a) Representative immunofluorescence images of aortic root greater curvature including staining for Vcam1, Cd36, VE-Cadherin, and combination

image. b) Representative immunofluorescence images of aortic root lesser curvature including staining for Vcam1, Cd36, VE-Cadherin, and combination image.

Supplemental Figure 10: Representative immunofluorescence images of transition zone between Vcam1-high region and Cd36-high region in the aortic root.